

SATELLITE OBSERVATIONS OF OCEANIC SHELF-SLOPE EXCHANGE

A Senior Thesis

By

Elizabeth Annah Jensen

1996-97 University Undergraduate Research Fellow

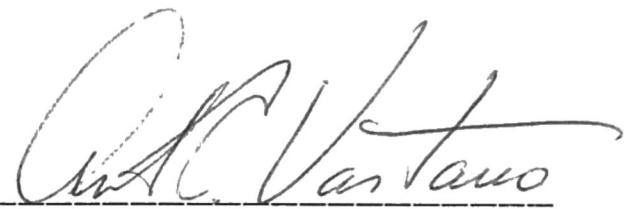
Texas A&M University

Group: Analysis

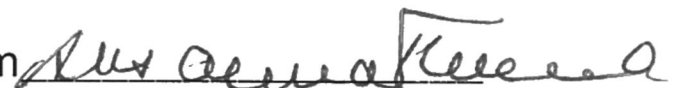
**SATELLITE OBSERVATIONS
OF
OCEANIC SHELF-SLOPE EXCHANGE**

Elizabeth Annah Jensen
University Graduate Research Fellow, 1996-97
Texas A&M University
Department of Oceanography

Undergraduate Advisor



Exec. Dir., Honors Program



Abstract

The transport of water masses and energy along and across the shelf edge has significance for both the abiotic and biotic components of local and distant regions of the Texas-Louisiana continental shelf in the northwestern Gulf of Mexico. Sequential Infrared images obtained by NOAA satellite Advanced Very High Resolution Radiometer (AVHRR) instruments have been used to examine the structure and assess motion of surface waters during episodic events at the shelf edge along the Brownsville Front. Transport seaward and shelfward is associated with the counter-clockwise rotation around the Texas Plume, a seaward extension of the Front in the vicinity of Alaminos Canyon. When it occurs, this feature is a spatially-localized dynamic event. Submesoscale, counter-clockwise rotating eddies have been observed arrayed along the Front from the longitude of Brownsville to that of Atchafalaya Bay. These features represent spatially sequential, advecting mixing mechanisms that translate *eastward* along the shelf edge and induce shelf-slope exchange. Larger, clockwise-rotating Loop Current eddies bring about converse exchange through their clockwise rotation as they move *westward* along the shelf edge. In circumstances where organized motion along the Brownsville Front is weak, exchange has been observed in terms of interlaced seaward and shelfward hammer-head formations that reach across the shelf edge. Without westward penetration of the Loop Current or a Loop Current eddy west of the Mississippi Delta's longitude, surface waters seaward of the Louisiana Bight are shown to move due south and reach the vicinity of Campeche Bank.

Introduction

The evolution of mesoscale and submesoscale features at and along the edge of the Texas-Louisiana Continental Shelf are contributing factors to the high biological, chemical and physical variability that characterizes this zone. Transitory current regimes import slope waters to the slope and conversely export shelf water to the oceanic environment. The mixing of water and the exchange of momentum along the shelf edge are the result of interactions between advective and turbulent events. Biological and chemical aspects of the shelf-slope region are also clearly influenced by these episodes and the associated turbulent diffusion of properties and contents.

Field investigations that include hydrographic surveys of waters in the shelf-slope region are traditional approaches to understanding the physical nature of water masses (Thurman, 1997). Estimates of exchange processes utilizing these data depend on the high information content of vertical property sections along ship track lines. This source has the potential to detect mesoscale features along the shelf edge and resolve submesoscale vertical structure. Satellites have shown the presence of features in horizontal distributions of sea surface temperature gathered by satellite infrared imagery (Vastano and Barron, 1994).

Research Problem

This Fellows research project focused on identification and analysis of physical phenomena along the edge of the Texas-Louisiana Continental

Shelf in an initial reconnaissance. As a result, six different cases were found that contained evidence for shelf-slope exchange. Flow patterns that demonstrated sea surface manifestations of the exchange processes were extracted from the satellite observations and several stream-function analyses were made to portray associated circulation tendencies.

Satellite Imagery

The present NOAA constellation of TIROS (**T**ele**v**ision and **I**n**f**ra**R**ed **O**bservation Satellite) satellites is part of an ongoing and near forty-year-long series of observations from polar-orbiting platforms initially meant for meteorological research. The instrument on these satellites used for the present oceanic study is the **A**dvanced **V**ery **H**igh **R**esolution **R**adiometer (AVHRR). This multi-spectral optical scanning device (Robinson, 1991) has five channels of approximately one kilometer by one kilometer spatial resolution. The satellite-recorded electromagnetic radiance values obtained in the AVHRR's 11 μm channel are the basis for estimates of the sea surface temperature (SST) structure. Temporal changes in SST distributions can be analyzed for estimates of surface motion and indications of dynamic processes.

Motion Analysis

The extraction of flow vectors from sequential infrared imagery (Vastano and Borders, 1984) is based on a conceptual framework that assumes the sea surface motion to be strictly two-dimensional with neg-

ligible contributions from horizontal waves or air-sea interaction (Vastano and Reid, 1985). Under such conditions, mean advective velocities over the time interval between the infrared images can be estimated with displacements of small scale perturbations on the mean temperature distribution. The method used in this work for identifying and measuring displacements is known as interactive feature tracking. Vastano and Barron (1994) have compared such satellite advective flow observations with those computed from coincident drifting buoy displacements in order to estimate accuracy. The inherent portion of any speed error is due to the finite or pixel structure of the AVHRR images and is 1.8 cm s^{-1} over twenty-four hours. The comparison study used image intervals of 23.9 hours and established a standard error in speed estimates of 5.5 cm s^{-1} with an azimuthal error of 1.7° over a speed range of 0-60 cm s^{-1} .

Case Studies

The six flow fields presented below contain two examples of the Texas Plume (Vastano, et al., 1995) extending seaward and southeastward at the shelf edge; southerly movement of the Mississippi River outflow off the shelf; two cases showing the influence of large eddy features moving along the shelf edge; and the flow produced at the shelf edge by the seaward penetration of counter-rotating, paired vortices. In the accompanying pictures lighter shades of gray indicate cooler surface waters.

Figure	Initial Image	Final Image
1 & 2	12/03/87	12/05/87
4	05/05/88	05/06/88
6	03/31/89	04/01/89
8	10/07/87	10/08/87
10	04/16/83	04/17/83
12	02/24/90	02/25/90

Mississippi River Outflow

The green vectors shown in Figure 1 show seaward motion of the Mississippi River's outflow from the Delta. The southerly movement of the river waters extends over a range of approximately sixty kilometers. Just south of 24.5° N, the plume reverses and the yellow vectors of Figure 2 indicate entrainment by the northeastward flow on the western, adjacent side of the Loop Current. Figure 3 provides streamfunction estimates that were computed for the plume by three day surface parcel trajectories holding the vector field constant.

Counter-clockwise eddy

Anticyclonic rotation around the eddy feature is illustrated by the green flow vectors in Figure 4. The continuation of the surface flow

regime to the east and southeast is shown by the white vectors. The rotational sense of the eddy and the Front are the same suggesting that continuous flow of the Front could be enveloping smaller cyclonic, turbulent features such as those within the regime and outlined in yellow and red.

Texas Plumes

Figures 6,7 and 8,9 present red flow vectors distributions and the associated streamfunction approximations for two examples of the cyclonic Texas Plume. The central regions of each plume are located over the lower portion of the continental slope near 93-94°W, 26.5°N. Both flow regimes extend seaward at the shelf break in the vicinity of 95°W, 27.5°N. This geographic position along the shelf edge is marked by a steep topographic gradient leading downslope into deeper waters.

Loop Current Eddy

The northern side of the eddy and a strong SST gradient overlies the edge of the continental shelf near 92°W, 28°N in Figures 10,11. The clockwise motion around the center is shown by red flow vectors. Note that the normal Brownsville Front flow regime has been reversed west of the eddy as motion is from east to west (green vectors) along the shelf break. Hereafter, the westward to southerly flow on the shelf edge is entrained into a counter-clockwise feature (yellow vectors) centered at 95.5°W, 26.5°N.

Paired Vortices

The paired vortices shown in Figure 12,13 are immediately south of the shelf break which is traced by the thin white line. They illustrate the direct seaward transfer of cooler shelf waters in the absence of the strong and organized eastward flow regime associated with the Brownsville Front. At the time of the satellite observations, the entire length of the shelf edge from latitude of Brownsville to the longitude of the Mississippi Delta was alternately crossed by the shoreward penetration of paired, warm vortices and their converse (Figure 12). The close association of these warm and cold features gave the appearance of their being interlaced and under an evolution giving rise to even smaller ones.

References

- Robinson, I. S. (1991) *Satellite Oceanography* Ellis Horwood Limited, first edition 1985 reprinted, 455 pp.
- Thurman, Harold V. (1997) *Introductory Oceanography* Prentice Hall, eighth edition, 544 pp.
- Vastano, Andrew C., Charlie N. Barron Jr, and Edwin W. Shaar Jr (1995) *Satellite Observations of the Texas Current* Cont. Shelf Res., V15, N6, pp. 729-754.
- Vastano, Andrew C. and Charlie N. Barron Jr (1994) *Satellite Observations*

of Surface Circulation in the Northwestern Gulf of Mexico during March and April, 1989 Cont. Shelf Res., V14, N6, pp.607-628.

Vastano, Andrew C. and R. O. Reid (1985) *Sea Surface Topography Estimation with Infrared Satellite Imagery* J. Atmos. Oceanic Tech., 2, 393-400.

Vastano, Andrew C. and S. E. Borders (1984) *Sea Surface Motion over an Anticyclonic Eddy on the Oyashio Front* Remote Sens. Environ., 16, 87-90.

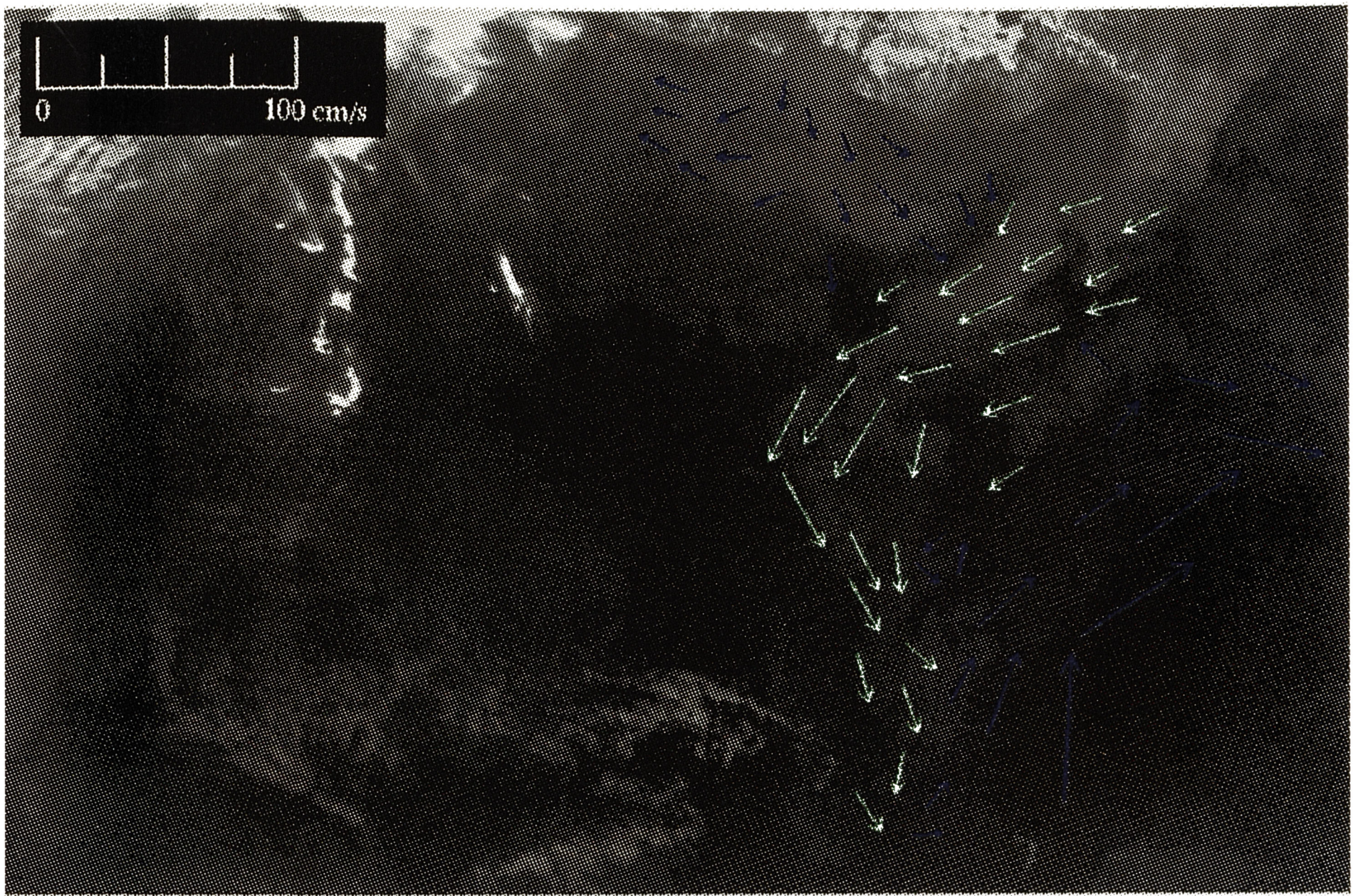


Figure 1 (above)

Figure 2 (below)

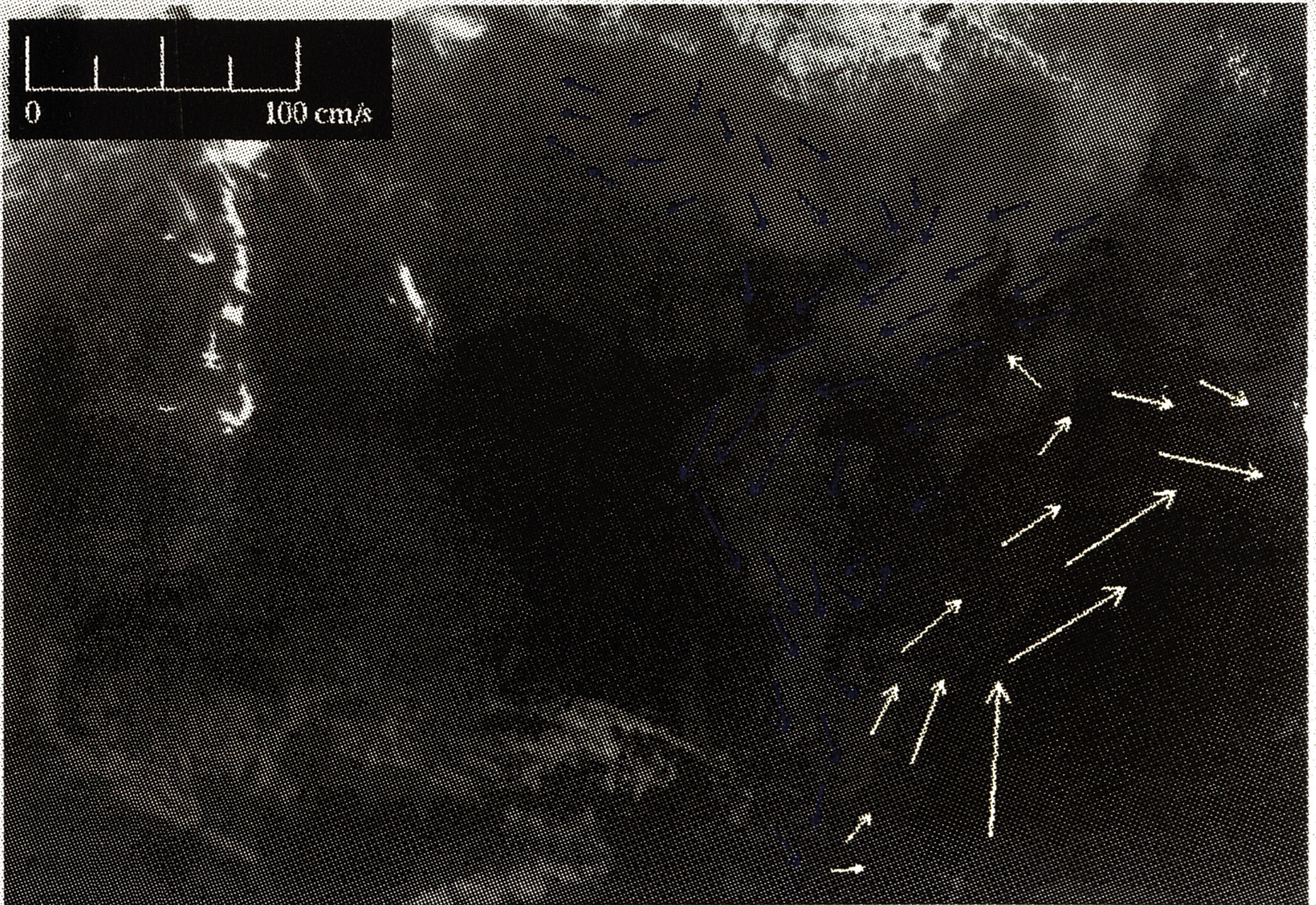


Figure 3

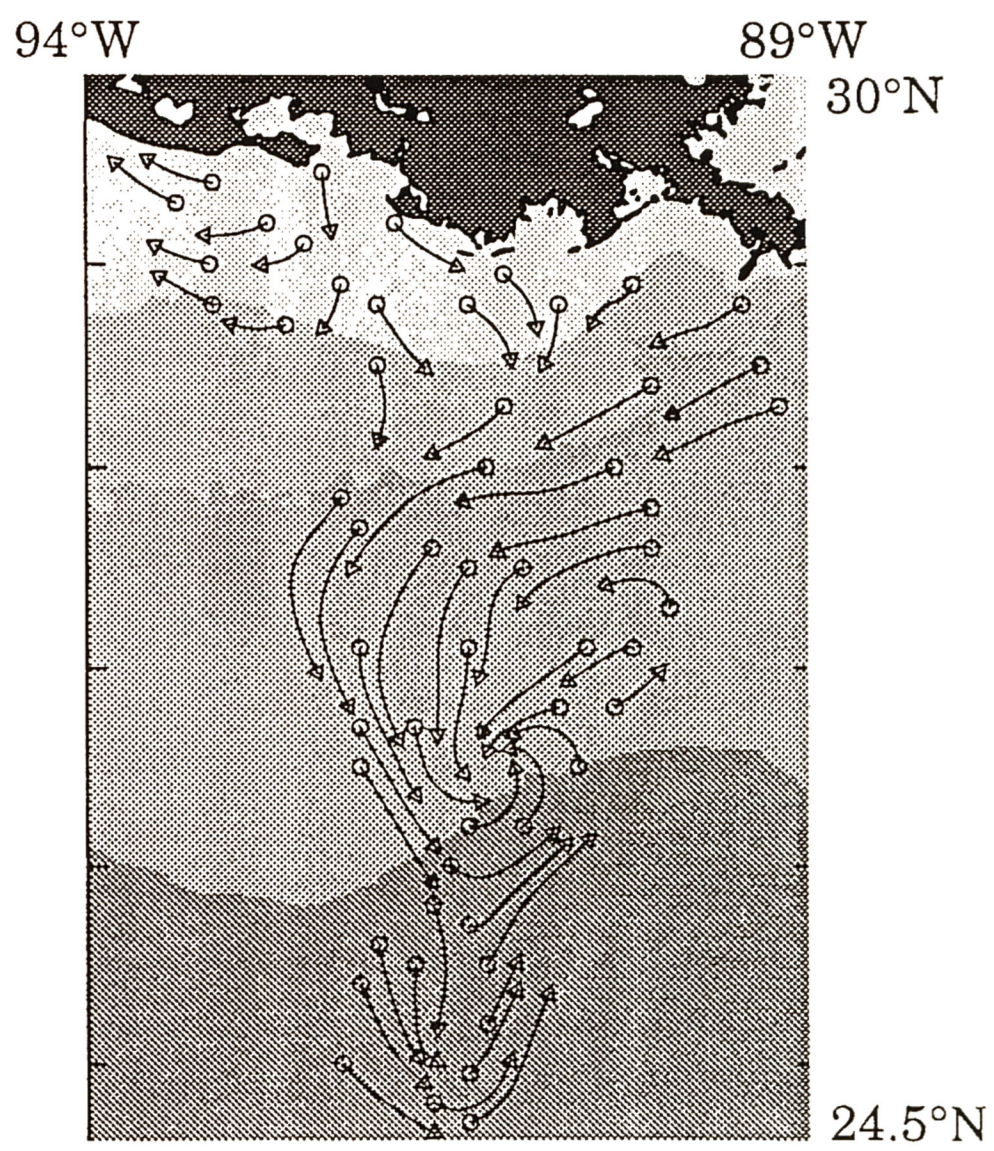


Figure 4

0 100 cm/s

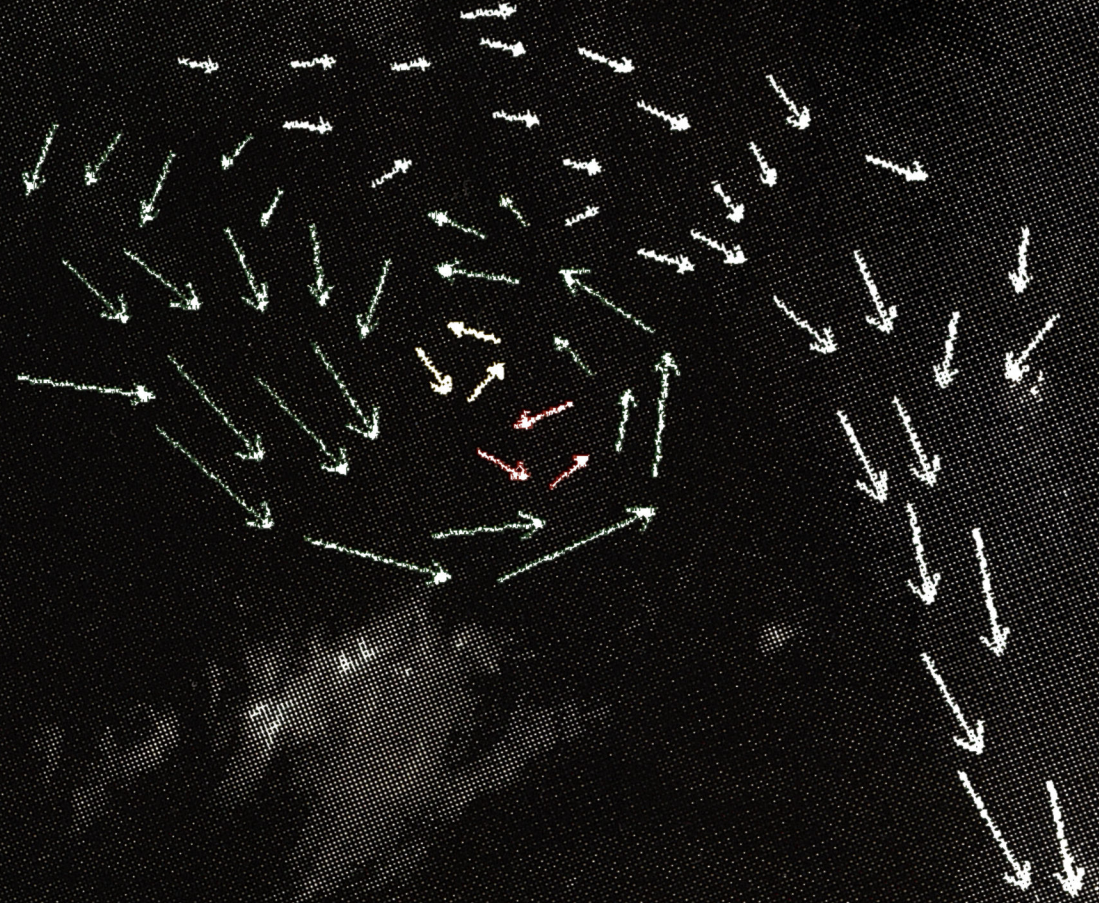
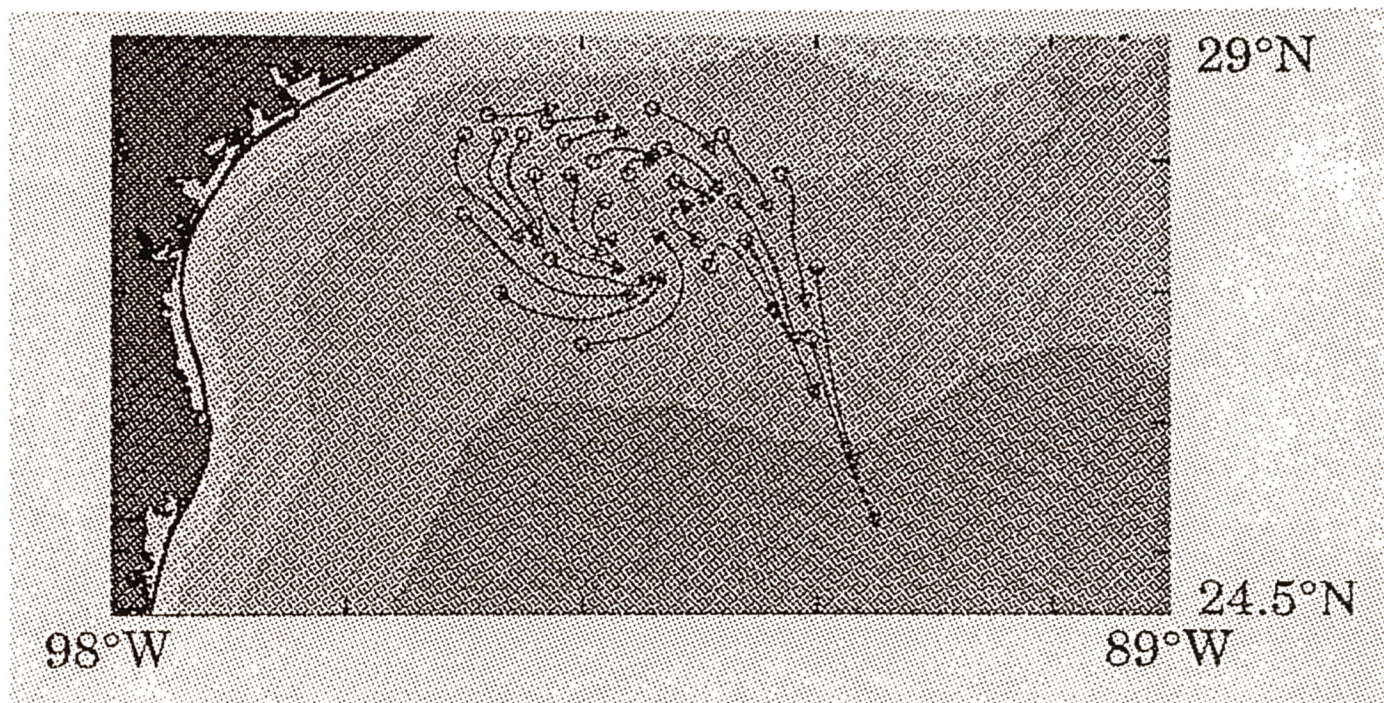


Figure 5



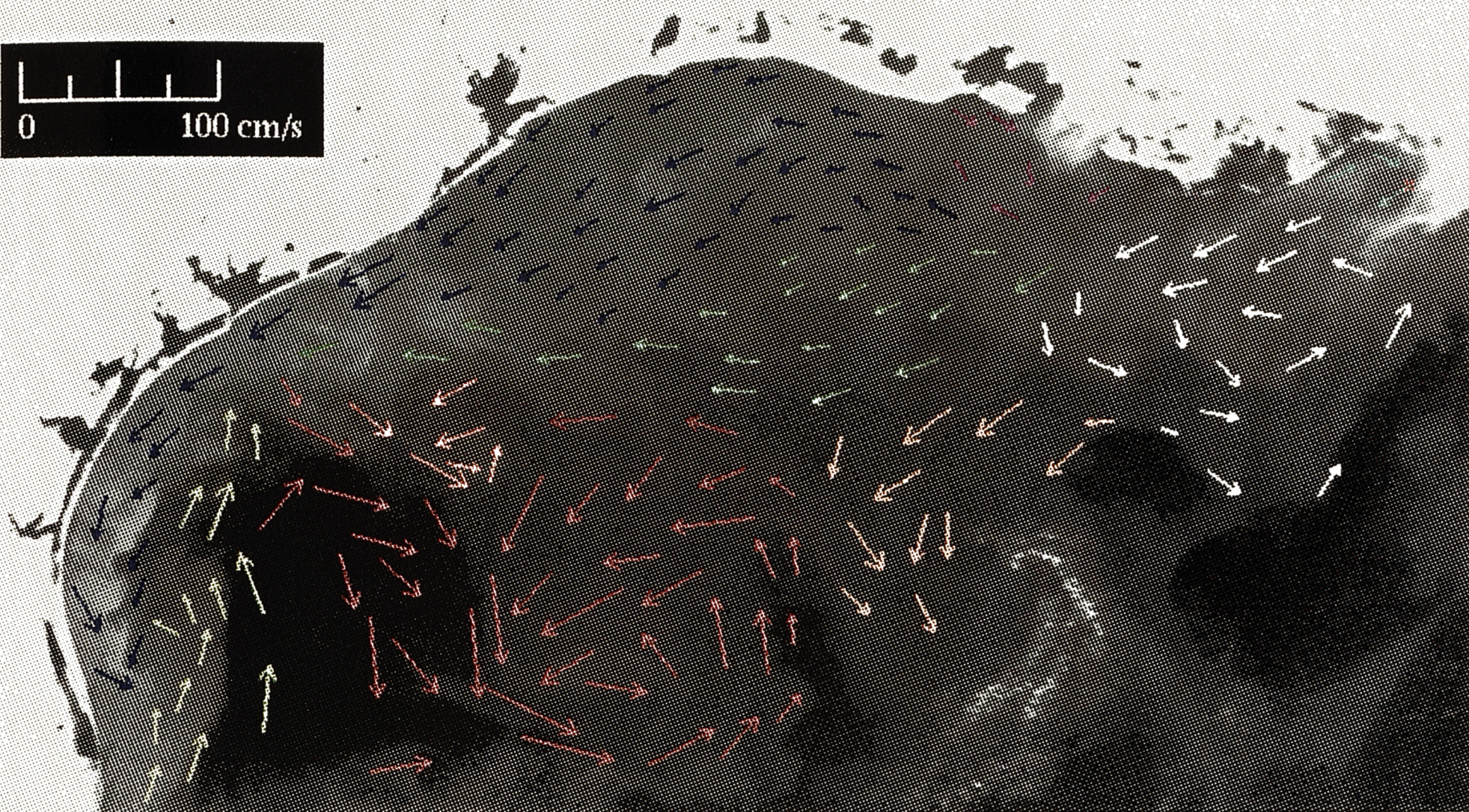
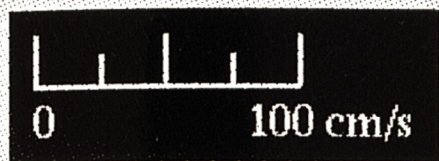
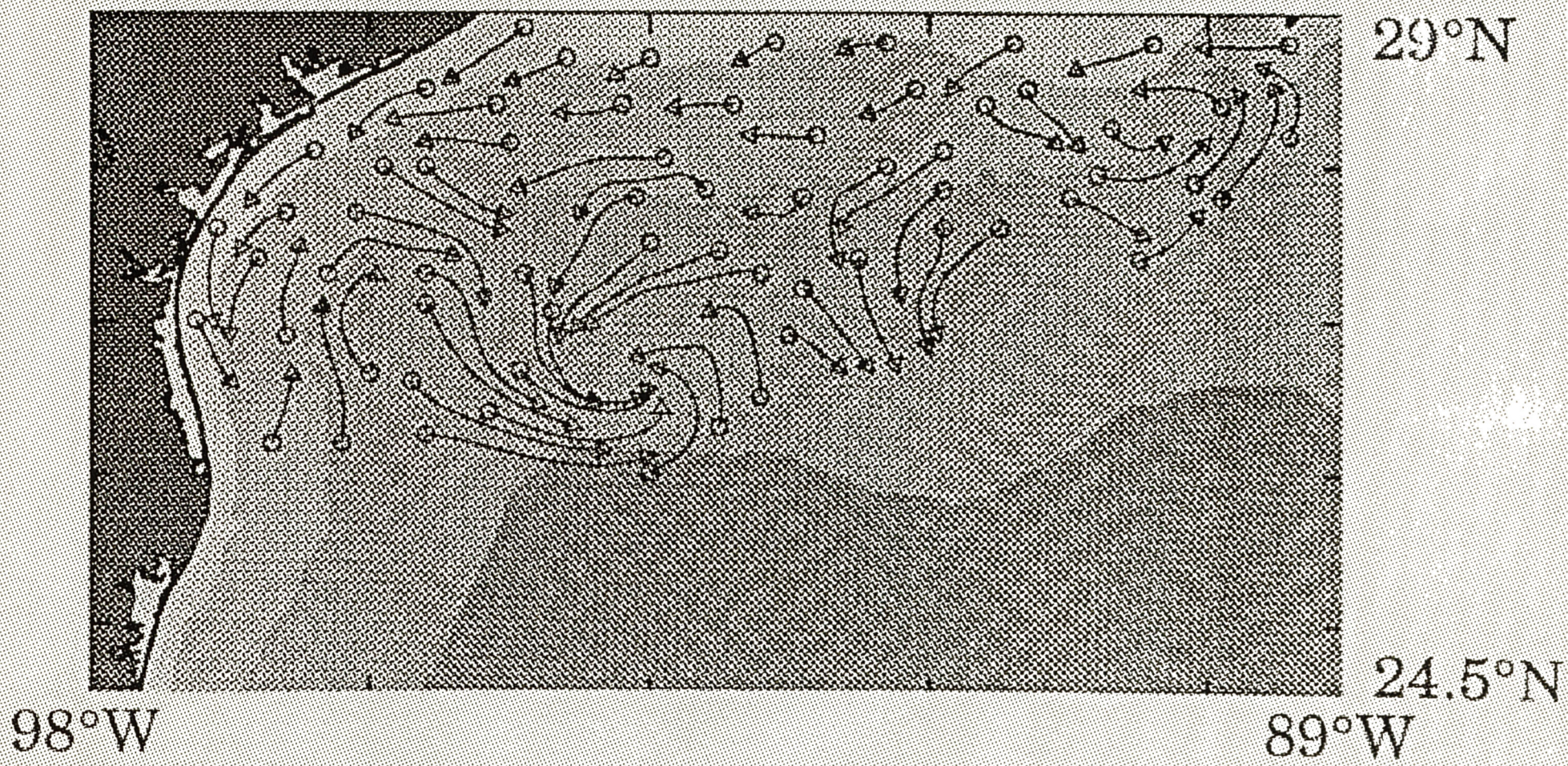


Figure 6 (above)

Figure 7 (below)



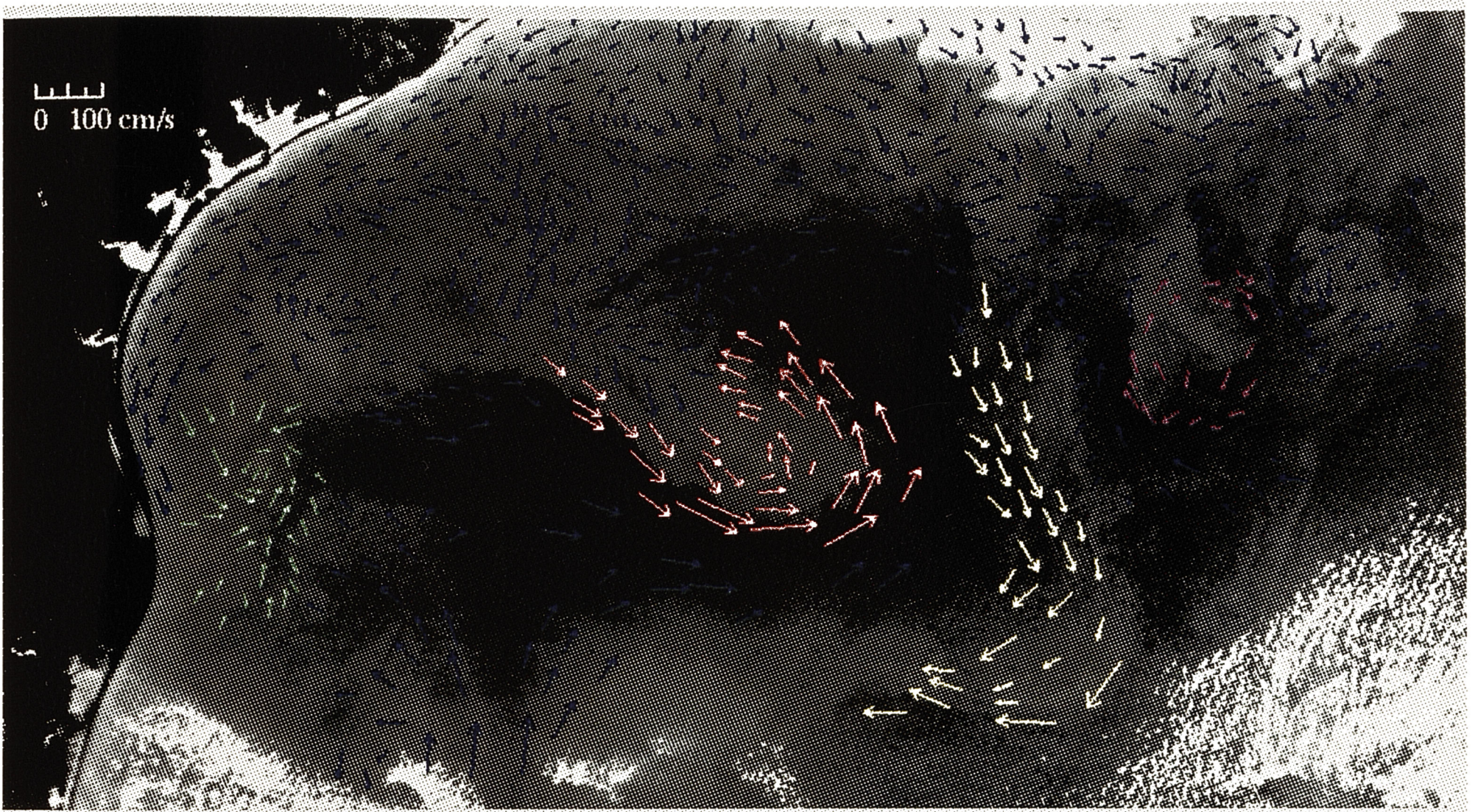
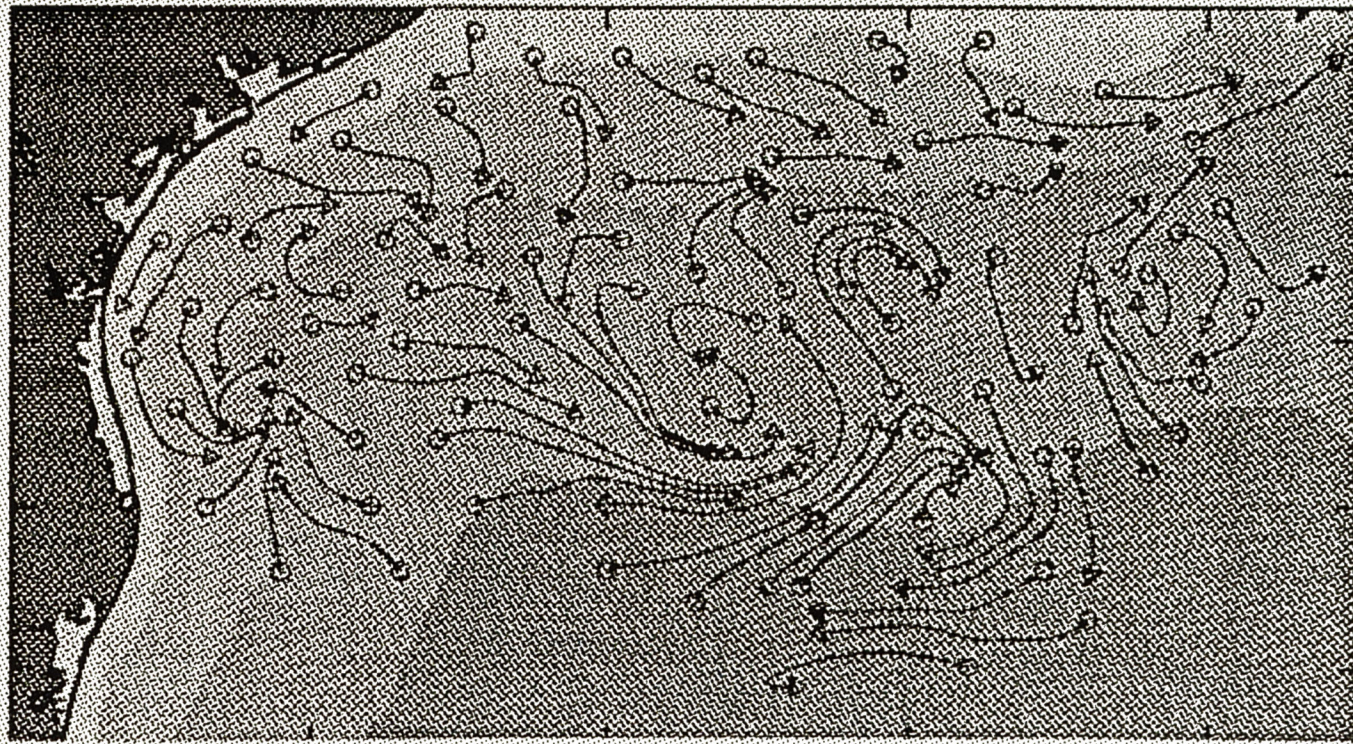


Figure 8 (above)

Figure 9 (below)



98°W

29°N

24.5°N

89°W

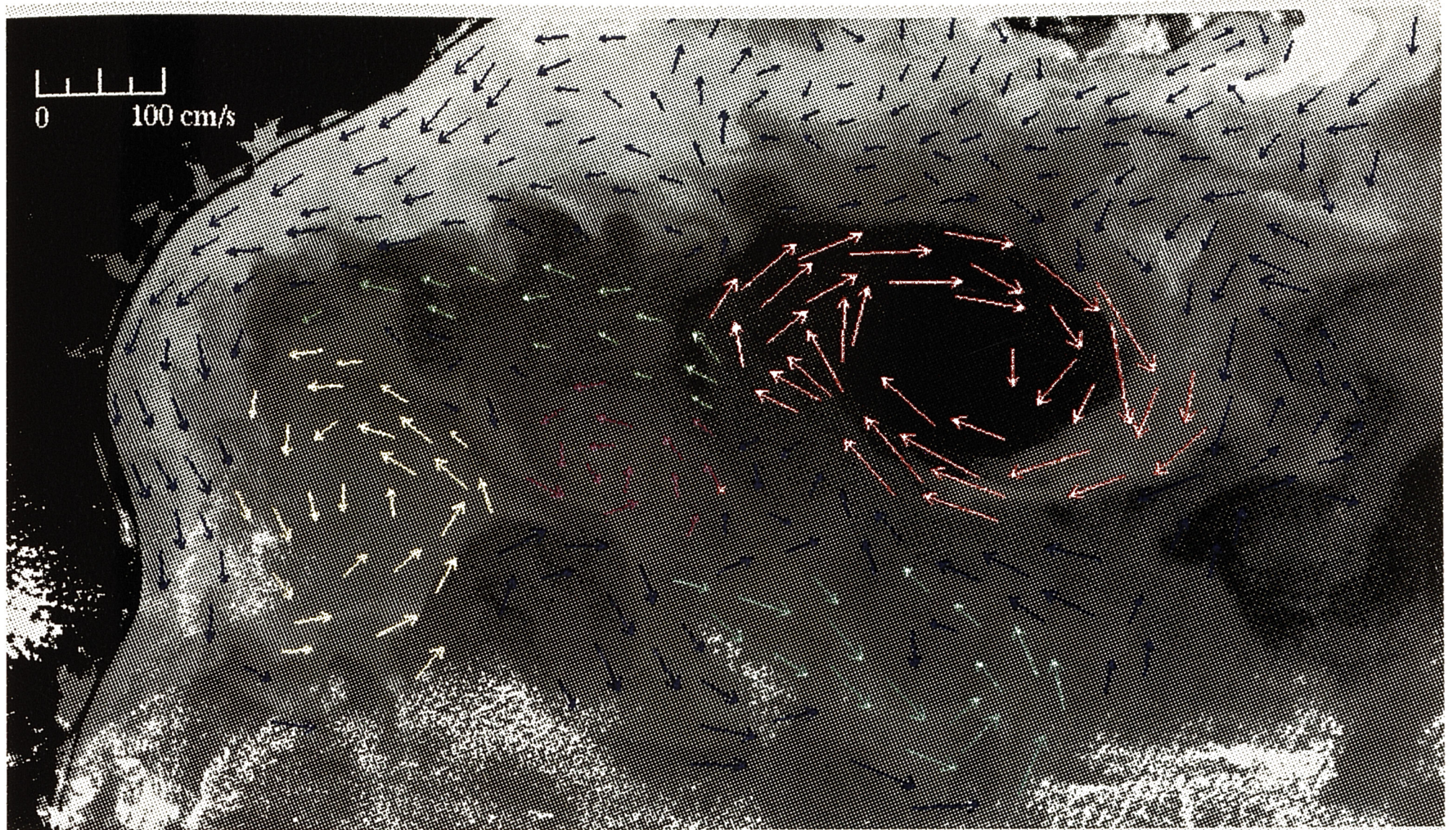
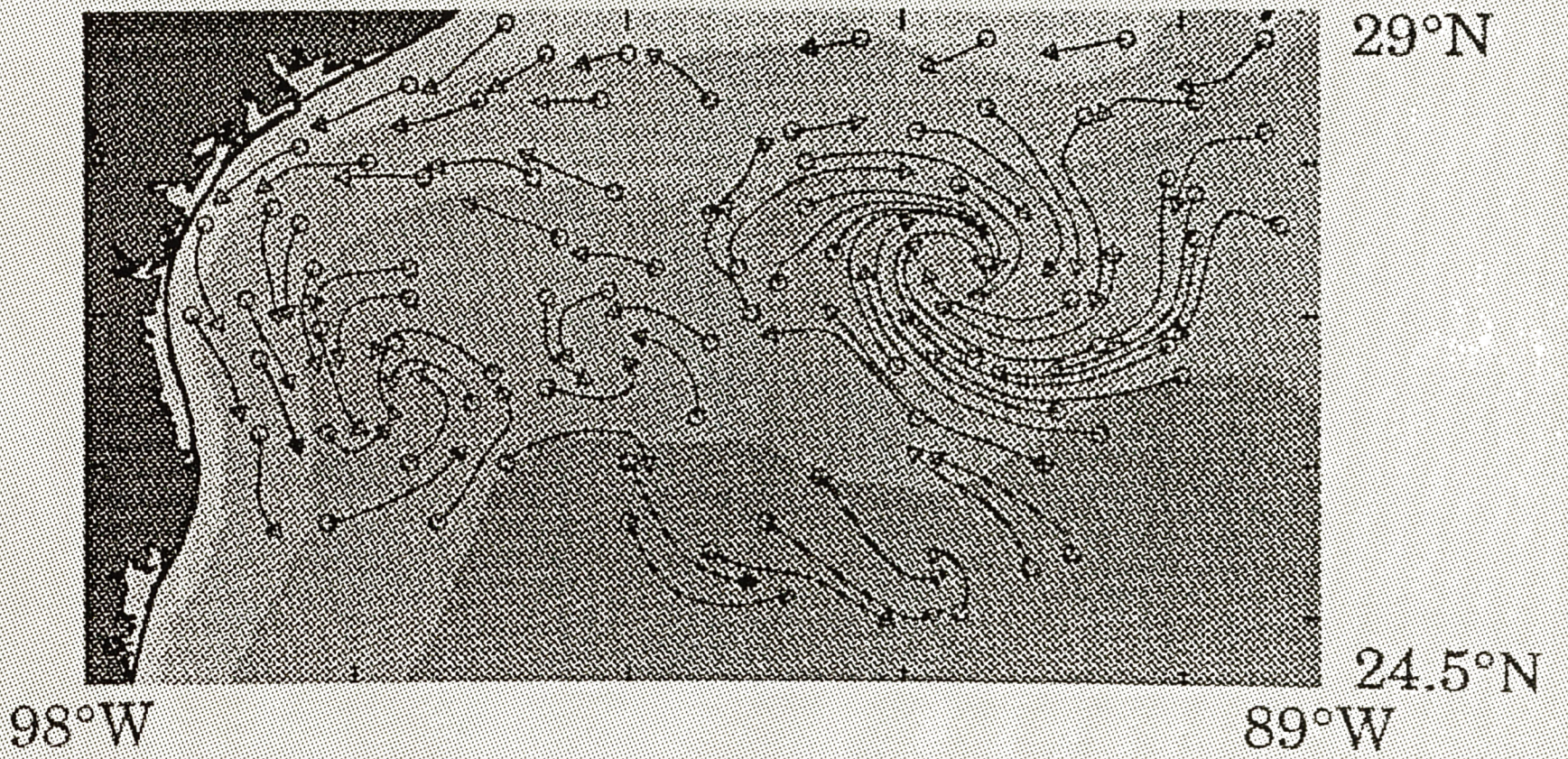


Figure 10 (above)

Figure 11 (below)



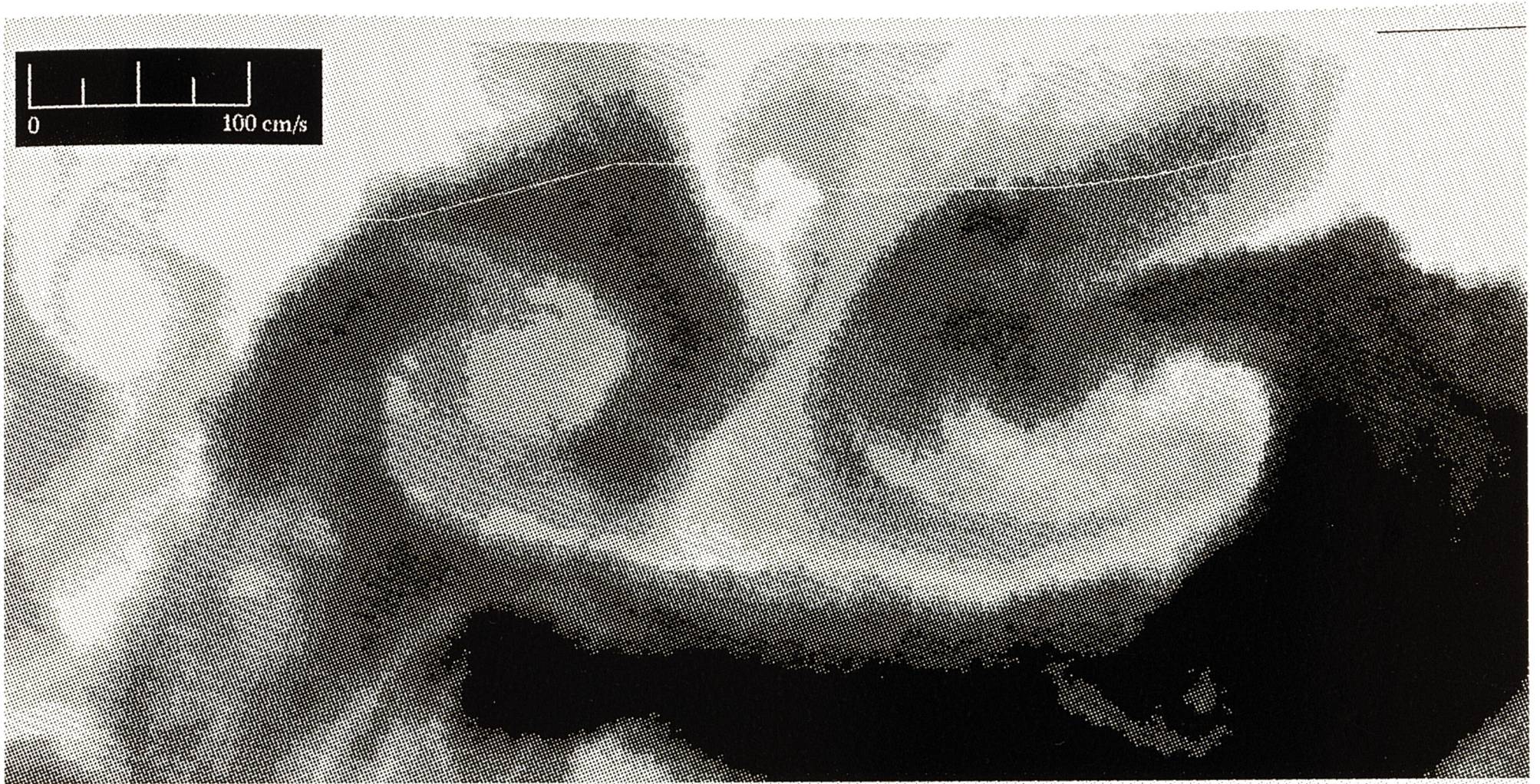


Figure 12 (above)

Figure 13 (right)

